Hindawi Publishing Corporation
Mathematical Problems in Engineering
Volume 2012, Article ID 867042, 18 pages
doi:10.1155/2012/867042

Research Article

Distinguishing Stationary/Nonstationary Scaling Processes Using Wavelet Tsallis q-Entropies

Julio Ramirez Pacheco,[1] Deni Torres Román,[2] and Homero Toral Cruz[3]

[1] *Department of Basic Sciences and Engineering, University of Caribe, 74528 Cancún, QROO, Mexico*
[2] *Department of Electrical Engineering, CINVESTAV-IPN Unidad Guadalajara, 45010 Zapopán, JAL, Mexico*
[3] *Department of Sciences and Engineering, University of Quintana Roo, 77019 Chetumal, QROO, Mexico*

Correspondence should be addressed to Julio Ramirez Pacheco, jramirez@ucaribe.edu.mx

Received 22 July 2011; Revised 17 October 2011; Accepted 25 October 2011

Academic Editor: Carlo Cattani

Classification of processes as stationary or nonstationary has been recognized as an important and unresolved problem in the analysis of scaling signals. Stationarity or nonstationarity determines not only the form of autocorrelations and moments but also the selection of estimators. In this paper, a methodology for classifying scaling processes as stationary or nonstationary is proposed. The method is based on wavelet Tsallis q-entropies and particularly on the behaviour of these entropies for scaling signals. It is demonstrated that the observed wavelet Tsallis q-entropies of $1/f$ signals can be modeled by sum-cosh apodizing functions which allocates constant entropies to a set of scaling signals and varying entropies to the rest and that this allocation is controlled by q. The proposed methodology, therefore, differentiates stationary signals from non-stationary ones based on the observed wavelet Tsallis entropies for $1/f$ signals. Experimental studies using synthesized signals confirm that the proposed method not only achieves satisfactorily classifications but also outperforms current methods proposed in the literature.

1. Introduction

The theory of scaling processes has shown to be meaningful in several fields of applied science [1]. Some aspects of scaling behaviour have been reported in finance [2, 3], in the analysis of heart rate variability and EEGs in physiology [4, 5], in the characterization of mood and other behavioural variables in psychology [6], in the modelling of computer network traffic and delays in LANs and WANs [7, 8], and in the study of the velocity field of turbulent flows in turbulence [9–12] among others. The scaling signals studied in these fields can be modelled by a wide variety of stochastic processes, the majority of which are characterized by the single scaling index α or the associated Hurst index H. Theoretically, the

scaling index α determines not only the nature of the signal in terms of smooth, stationarity, nonstationarity, and correlations but also the selection of the methodologies employed to estimate α. The boundary $\alpha = 1$ is of special importance since processes for which $\alpha < 1$ are categorized as stationary in the sense that their statistical properties are invariant to translations and processes with $\alpha > 1$ are non-stationary. The stationary/non-stationary condition is fundamental for analysis and estimation purposes as many estimators have been devised for stationary signals while others have been formulated for non-stationary ones. The application of a non-stationary signal to an analysis/estimation technique designed to work in stationary conditions will result in an ambiguous analysis/estimate. For a review on the methodologies used to estimate α and the range of the scaling index over which they are applicable please refer to the work of Serinaldi [13], Malamud and Turcotte [14], and Gallant et al. [15]. In practice, a scaling process analyst does not known apriori the nature of the signal, and usually the estimation of α is performed somewhat arbitrarily without a stage of signal classification. Many articles in the literature, claiming that a given phenomena can be modelled by scaling signals, have performed the estimation of α without a phase of signal classification, and therefore their results remain questionable. Moreover, the scaling property of signals, in particular the long-memory characteristic, can also be caused by structural breaks in the mean, a common non-stationarity embedded in the signal [16, 17]. Because of this, the phase of signal classification is not only important but also necessary. The phase of signal classification was first recognized as important by Eke and coworkers in physiological signal analysis [4–6]. In their work, Eke et al. emphasized the importance of signal classification, the implications of omitting this phase, and the necessity of including this phase as a first step for enhancing the estimation and analysis of scaling signals. They claimed that by integrating this step in the traditional estimation and analysis methodologies, significant improvements can be achieved, and the possibility of misinterpreting the phenomena is decreased. Traditionally, signal classification has been performed by methods based on PSD [5, 6] on fractional Brownian motions, fBms, and fractional Gaussian noises, fGns. The characteristics of fBms and fGns, however, are visually different, and the signal classification process can even be performed by eye. Motivated by this, the present paper not only extends the results presented in [5] for the case of PPL signals but also proposes a methodology based on wavelet Tsallis q-entropies to differentiate scaling processes as stationary or non-stationary. The method is based on the observed sum-cosh window behaviour of these entropies which allocates constant entropies to stationary signals and varying entropies to non-stationary ones reducing the classification process to the constant/nonconstant character of the observed estimated entropies of the signals under study. Experimental and comparison studies not only confirm the capabilities of the method but also their advantages over standard methodologies based on PSD. The remainder of the paper is structured as follows. Section 2 provides a brief review of scaling processes, their definitions, and some standard results concerning its wavelet analysis. Section 3 describes wavelet entropies and its applications and derives the sum-cosh window behaviour observed in wavelet Tsallis q-entropies for signals with $1/f^{\alpha}$ behaviour. The techniques employed for classifying scaling signals as stationary or non-stationary as well as their advantages and disadvantages are briefly reviewed in Section 4 along with a description of the proposed methodology based on wavelet Tsallis q-entropies to discriminate signals. Section 5 describes the methodology used in the paper for testing the accuracy and robustness of the proposed technique and also details the comparative study to be performed among the techniques used for scaling signal classification. Section 6 presents the experimental results, and finally the conclusions of the paper are drawn in Section 7.

2. Wavelet Analysis of Scaling Processes

2.1. Scaling Processes

Scaling processes of parameter α, also called $1/f^{\alpha}$ or power-law processes, have been extensively applied and studied in the scientific literature since they model diverse phenomena [2, 3] within these fields. These processes are sufficiently characterized by the parameter α, called the scaling-index, which determines many of their properties. Various definitions have been proposed in the scientific literature, some based on their characteristics such as self-similarity or long memory, others based on the behaviour of their PSD. In this paper, a scaling process is a random process for which the associated PSD behaves as a *power law* in a range of frequencies [8, 9], that is,

$$S(f) \sim c_f |f|^{-\alpha}, \quad f \in (f_a, f_b), \tag{2.1}$$

where c_f is a constant, $\alpha \in \mathbb{R}$ the *scaling* index, and f_a, f_b represent the lower and upper bound frequencies upon which the power-law scaling holds. Depending upon f_a, f_b, and α, several particular scaling processes and behaviours can be identified. Independently of α, local regularity and band-pass power-law behaviour are observed whenever $f_a \to \infty$ and $f_b > f_a \gg 0$, respectively. When the scaling-index α is taken into consideration, long-memory behaviour is observed when both $0 < \alpha < 1$ and $f_b > f_a \to 0$. Self-similar features (in terms of distributional invariance under dilations) are observed in all the scaling-index range for all f. Scaling-index α determines not only the stationary and non-stationary condition of the scaling process but also the smoothness of their sample path realizations. The greater the scaling index α, the smoother their sample paths. As a matter of fact, as long as $\alpha \in (-1, 1)$, the scaling process is stationary (or stationary with long memory for small f and $\alpha \in (0, 1)$) and non-stationary when $\alpha \in (1, 3)$. Some transformations can make a stationary process appear non-stationary and vice versa. Outside the range $\alpha \in (-1, 3)$, several other processes can be identified, for example, the so-called extended fBms and fGns defined in the work of Serinaldi [13]. The persistence of scaling processes can also be quantified by the index α, and within this framework, scaling processes possess negative persistence as long as $\alpha < 0$, positive weak long persistence when $0 < \alpha < 1$, and positive strong long persistence whenever $\alpha > 1$. Scaling signals encompasses a large family of well-known random signals, for example, fBms, fGns [18], pure power-law processes [9], multifractal processes [8], and so forth. FBm, $B_H(t)$, comprises a family of Gaussian, self-similar processes with stationary increments, and because of the Gaussianity, it is completely characterized by its autocovariance sequence ACVS, which is given by

$$\mathbb{E}B_H(t)B_H(s) = R_{B_H}(t, s) = \frac{\sigma^2}{2}\left\{|t|^{2H} + |s|^{2H} - |t - s|^{2H}\right\}, \tag{2.2}$$

where $0 < H < 1$ is the Hurst-index. FBm is non-stationary, and as such no spectrum can be defined on it; however, fBm possesses an average spectrum of the form $S_{\text{fBm}}(f) \sim c|f|^{-(2H+1)}$ as $f \to 0$ which implies that $\alpha = 2H+1$ [19]. FBm has been applied very often in the literature; however it is its related process, fGn, which has gained widespread prominence because of the stationarity of its realizations.

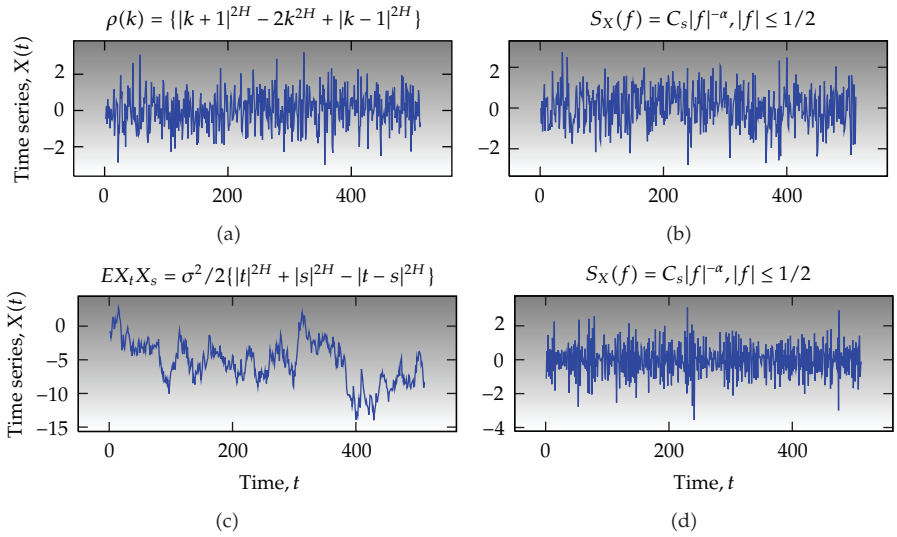

Figure 1: Sample path realizations of some scaling processes. Top left depicts a fGn with $\alpha = -0.1$, top right a PPL process with $\alpha = -0.1$, bottom left plot a fBm signal with $\alpha = 1.9$, and finally bottom right plot a PPL process with $\alpha = 1.9$.

FGn, $G_{H,\delta}(t)$, obtained by sampling a fBm process and computing increments of the form $G_{H,\delta}(t) = 1/\delta\{B_H(t+\delta) - B_H(t)\}$, $\delta \in \mathbb{Z}_+$ (i.e., by differentiating fBm), is a well-known Gaussian process. The ACVS of this process is given by

$$\mathbb{E}G_{H,\delta}(t)G_{H,\delta}(t+\tau) = \frac{\sigma^2}{2}\left\{|\tau+\delta|^{2H} + |\tau-\delta|^{2H} - 2|\tau|^{2H}\right\}, \tag{2.3}$$

where $H \in (0,1)$ is the Hurst-index. The associated PSD of fGn is given by [9]

$$S_{\text{fGn}}(f) = 4\sigma_X^2 C_H \sin^2(\pi f) \sum_{j=-\infty}^{\infty} \frac{1}{|f+j|^{2H+1}}, \quad |f| \leq \frac{1}{2}, \tag{2.4}$$

where σ_X is the process' variance and C_H is a constant. FGn is stationary and for large enough τ and under the restriction of $1/2 < H < 1$ possesses long-memory or long-range dependence (LRD). The scaling index α associated to fGn signals is given by $\alpha = 2H - 1$ as its PSD, given by (2.4), behaves asymptotically as $S_{\text{fGn}}(f) \sim c|f|^{-2H+1}$ for $f \to 0$. Another scaling process of interest is the family of discrete pure power-law processes (dPPL) which are defined as processes for which their PSD behaves as $S_X(f) = C_S|f|^{-\alpha}$ for $|f| \leq 1$, where $\alpha \in \mathbb{R}$ and C_s represent a constant. PPL signals are stationary when the power-law parameter $\alpha < 1$ and non-stationary whenever $\alpha > 1$. As stated in the work of Percival [9], the characteristics of these processes and those of fBms/fGns are similar; however, the differences between fBms and PPLs with $\alpha > 1$ are more evident. As a matter of fact, differentiation of stationarity/non-stationarity is far more difficult for PPL than for fBms/fGns. Figure 1 displays some realizations of fGn, fBm, and PPL processes. The scaling-index α of the PPL signals is identical to the scaling-index of the associated fGn and fBm. Note that the characteristics of the sample paths of fGn are fairly different from those of fBm. In the case of PPL processes, this differentiation

is not so evident, and as a matter of fact when the scaling indexes approach the boundary $\alpha = 1$, classification becomes complex. For further information on the properties, estimators, and analysis techniques of scaling processes please refer to [2, 3, 8–10, 13, 14].

2.2. Wavelet Analysis of Scaling Signals

Wavelets and wavelet transforms have been applied for the analysis of deterministic and random signals in almost every field of science [20–22]. The advantages of wavelet analysis over standard techniques of signal analysis have been widely reported and its potential for non-stationary signal analysis proven. Wavelet analysis represents a signal X_t in time-scale domain by the use of an analyzing or mother wavelet, $\varphi_o(t)$ [23]. For the purposes of the paper, $\varphi_o(t) \in L_1 \cap L_2$ and the family of shifted and dilated $\varphi_o(t)$ form an orthonormal basis of $L_2(\mathbb{R})$. In addition, the finiteness of the mean average energy ($\mathbb{E}\int |X(u)|^2 du < \infty$) on the scaling process allows to represent it as a linear combination of the form:

$$X_t = \sum_{j=1}^{L} \sum_{k=-\infty}^{\infty} d_X(j,k)\varphi_{j,k}(t), \tag{2.5}$$

where $d_X(j,k)$ is the DWT of X_t and $\{\varphi_{j,k}(t) = 2^{-j/2}\varphi_o(2^{-j}t - k),\ j,k \in \mathbb{Z}\}$ is a family of dilated (of order j) and shifted (of order k) versions of $\varphi_o(t)$. The coefficients $d_X(j,k)$ in (2.5), obtained by DWT, represent a random process for every j, a random variable for fixed j and k, and as such many statistical analyses can be performed on them. Equation (2.5) represents signal X_t as a linear combination of L detail signals, obtained by means of the DWT. DWT is related to the theory of multiresolution signal representation (MRA), in which signals (or processes) can be represented at different resolutions based on the number of detail signals added to the low-frequency approximation signal. Detail random signals ($d_X(j,k)$) are obtained by projections of signal X_t into wavelet spaces $\mathcal{W}_j$, and approximation coefficients ($a_X(j,k)$) are obtained by projections of X_t into related approximation spaces $\mathcal{V}_j$. In the study of scaling processes, wavelet analysis has been primarily applied in the estimation of the wavelet variance [20, 24]. Wavelet variance or spectrum of a random processes accounts for computing variances of wavelet coefficients at each scale. Wavelet variance not only has permitted to propose estimation procedures for the scaling-index α but also to compute entropies associated with the scaling signals. Wavelet spectrum has also been used for detecting nonstationarities embedded in Internet traffic [20]. For stationary zero-mean processes, wavelet spectrum is given by

$$\mathbb{E}d_X^2(j,k) = \int_{-\infty}^{\infty} S_X\left(2^{-j}f\right)\left|\Psi(f)\right|^2 df, \tag{2.6}$$

where $\Psi(f) = \int \varphi(t)e^{-j2\pi ft}dt$ is the Fourier integral of $\varphi_o(t)$ and $S_X(\cdot)$ represents the PSD of X_t. Table 1 summarizes the wavelet spectrum for some standard scaling processes. For further details on the analysis, estimation, and synthesis of scaling processes please refer to the works of Abry and Veitch [23] and Bardet [25] and references therein.

Table 1: Wavelet spectrum or wavelet variance associated with different types of *scaling* processes. $\mathbb{E}(\cdot)$, $\mathrm{Var}(\cdot)$, and $\Psi(\cdot)$ represent expectation, variance, and Fourier integral operators, respectively.

Type of scaling process	Associated wavelet spectrum or variance
Long-memory process of index α	$\mathbb{E}d_X^2(j,k) \sim 2^{j\alpha}C(\psi,\alpha)$, $C(\psi,\alpha) = c_\gamma \int \lvert f\rvert^{-\alpha}\lvert\Psi(f)\rvert^2 df$
Self-similar process of index H	$\mathbb{E}d_X^2(j,k) = 2^{j(2H+1)}\mathbb{E}d_X^2(0,k)$
Hsssi process of index H	$\mathrm{Var}\, d_X^2(j,k) = 2^{j(2H+1)}\,\mathrm{Var}\, d_X(0,0)$
Pure power-law process of index α	$\mathbb{E}d_X^2(j,k) = C2^{j\alpha}$

3. Wavelet-Based q-Entropies

The concept of entropy has traditionally been employed to measure the information content of random signals and systems [26, 27]. Recently, entropic functionals, such as Shannon, Rényi, and Tsallis, have been extensively applied to quantify the complexities associated with random and nonlinear phenomena [28]. Information planes, which consist of the product of positive measures of entropic functional and the Fisher information (and also of entropy/disequilibrium product), are now being applied in numerous systems (e.g., atomic, molecular, geophysical, etc.). Entropic quantities involve the calculation of functionals on probability densities or probability mass functions (pmf). Depending upon the domain in which the pmfs are obtained, entropies usually inherit their name. Entropies are called spectral entropies when entropic functionals are applied to pmfs derived from the Fourier spectrum representation of the process. When the densities are determined in the time-scale domain by discrete wavelet transformations, the associated entropy functionals are called wavelet entropies [29, 30]. If the pmf is obtained via the continuous wavelet transform, CWT, the entropy is called continuous multiresolution entropy (CMqE) [31]. Wavelet Shannon entropy, tantamount to computing a Shannon entropy functional on a *pmf* derived from the wavelet variance, has found applications in event-related potentials in neuroelectrical signals [32, 33], structural damage identification [34], segmentation of EEG signals [35], characterization of complexity in random signals [36–38] among others. Entropic measures of order q (hereafter q-entropies) generalize Shannon entropy and provide the flexibility of fine tuning to a desired behaviour with the value of q. The pmf in time-scale domain for which all entropies in this paper are computed is obtained by

$$p_j = \frac{1/N_j \sum_k \mathcal{F}(d_X(j,k))}{\sum_{i=1}^{\log_2(N)} \{1/N_i \sum_k \mathcal{F}(d_X(j,k))\}}, \tag{3.1}$$

where $\mathcal{F}(\cdot)$ represents the variance or second-order moment of the $d_X(j,k)$, N_j (resp., N_i) stands for the total number of wavelet coefficients at scale j (resp., i), and N is the length of the process. For signals with $1/f$ PSD, the so-called wavelet spectrum-based pmf is determined by direct substitution of the wavelet spectrum of the process under study (see Table 1) into (3.1), which results in

$$p_j = 2^{(j-1)\alpha}\frac{1-2^\alpha}{1-2^{\alpha M}}, \tag{3.2}$$

where $M = \log_2(N)$. The density given in (3.2) represents the probability that the energy of the scaling signal is located at scale j. The pmf of (3.2) can be used to compute numerous information theoretic functionals such as entropies, Fisher information, and information planes. Zunino and coworkers computed Shannon entropy functional on (3.2) and called it wavelet entropy. Later explicit formulas for wavelet Rényi and Tsallis entropies were derived and some applications suggested. Normalized Shannon entropy functional of scaling signals is given by

$$\widehat{\mathscr{H}}(p) = \frac{1}{\log_2(M)}\left\{\frac{\alpha}{1-2^{-\alpha}} - \frac{\alpha M}{1-2^{-\alpha M}} - \log_2\left(\frac{1-2^{\alpha}}{1-2^{\alpha M}}\right)\right\}, \tag{3.3}$$

where $M = \log_2(N)$. Wavelet Rényi q-entropies, as in the case of Shannon entropies, are extensive entropies in the sense that for any two independent random variables X_1 and X_2, the joint entropy $\mathscr{H}_q^R(X_1, X_2) = \mathscr{H}_q^R(X_1) + \mathscr{H}_q^R(X_2)$. For scaling signals, Rényi entropy functional, $\widehat{\mathscr{H}}_q^R(p) = 1/(1-q)\log_2(\sum_j {p_j}^q)$, results in

$$\widehat{\mathscr{H}}_q^R(p) = \frac{q}{1-q}\left(\log_2\left(\frac{1-2^{\alpha}}{1-2^{\alpha M}}\right) - \frac{1}{q}\log_2\left(\frac{1-2^{\alpha q M}}{1-2^{\alpha q}}\right)\right), \tag{3.4}$$

where $q \in \mathbb{R}$ denotes the extensivity parameter. *Tsallis* q-entropies are nonextensive entropies in the sense that the extensivity property no longer holds. For a pmf p_j it is defined as

$$\widehat{\mathscr{H}}_q^T(p) = -\sum_{j=1}^{M} p_j^q \ln_q(p_j), \tag{3.5}$$

where $\ln_q(x) := (x^{1-q} - 1)/(1-q)$ is the q-logarithm function and $q \in \mathbb{R}$ the nonextensivity parameter. Tsallis entropies provide a valuable and interesting tool for the analysis of systems with long-range interactions, long memories, and so forth. The application of Tsallis entropies is vast, from the characterization of complexities in EEG signals [28] to the study of nonlinear systems [31]. Normalized Tsallis functional applied to (3.2) results in wavelet Tsallis q-entropies which is given by

$$\widehat{\mathscr{H}}_q^T(p;\alpha) = c_{M,q}\left\{1 - \left(\frac{1-2^{\alpha}}{1-2^{\alpha M}}\right)^q \left(\frac{1-2^{\alpha q M}}{1-2^{\alpha q}}\right)\right\} \tag{3.6}$$

$$= c_{M,q}\left\{1 - \left(\frac{\sinh(\alpha \ln 2/2)}{\sinh(\alpha \ln 2M/2)}\right)^q \left(\frac{\sinh(\alpha q M \ln 2/2)}{\sinh(\alpha q \ln 2/2)}\right)\right\} \tag{3.7}$$

$$= c_{M,q}\left\{1 - \frac{\mathrm{P}^{M-1}(2\cosh(\alpha q \ln 2/2))}{\left(\mathrm{P}^{M-1}(2\cosh(\alpha \ln 2/2))\right)^q}\right\}, \tag{3.8}$$

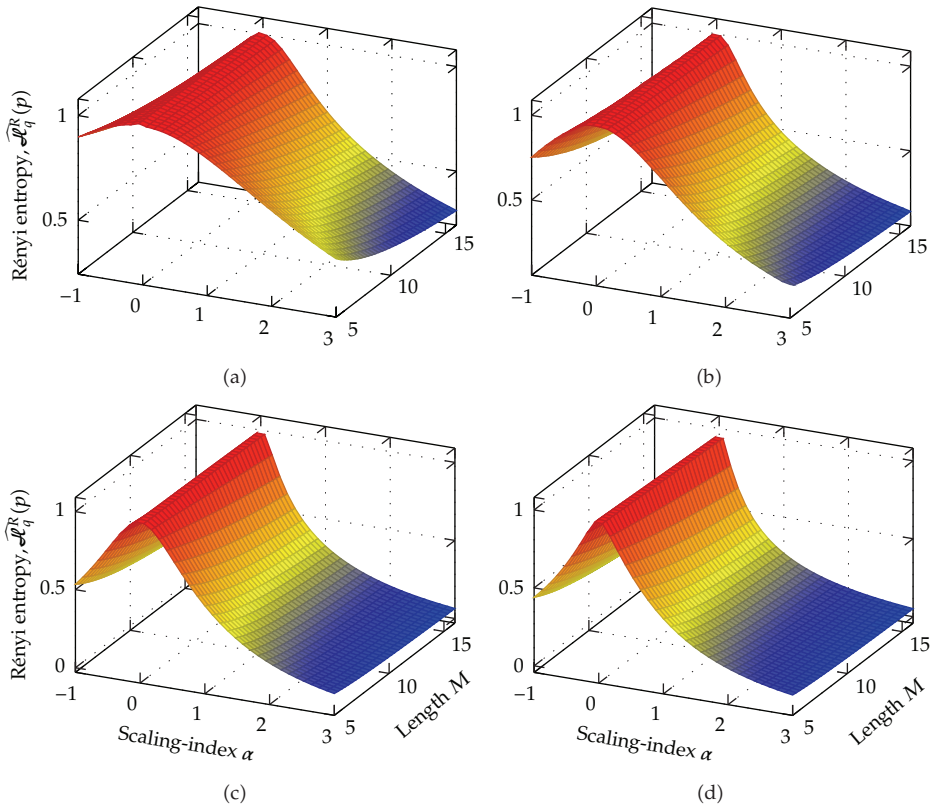

Figure 2: Wavelet Rényi q-entropies of $1/f$ signals. Top left plot computed with $q = 0.4$, top right plot with $q = 1.1$, bottom left plot with $q = 4$, and finally bottom right plot with $q = 15$.

where $c_{M,q} = 1/(1-M^{1-q})$ is a normalizing factor and $P^{M-1}(2\cosh u)$ is a polynomial of order $M-1$, that is,

$$P^{M-1}(\cdot) = (2\cosh u)^{M-1} - \frac{(M-2)}{1!}(2\cosh u)^{M-3} + \frac{(M-3)(M-4)}{2!}(2\cosh u)^{M-5} - \cdots. \tag{3.9}$$

Figure 2 displays the wavelet Rényi q-entropies of scaling processes. Note that independently of signal length, wavelet Rényi entropies display a bell-shaped form for these processes. Parameter q stretches the bell-shaped form as q is varied. Parameter q has, in view of these entropy planes, no effect on the form of the observed entropies as the bell-shaped form is maintained. The maximum entropy is achieved when the scaling process is a pure white noise ($\alpha = 0$), and as the process becomes non-stationary their entropies decrease. The form and behaviour of these entropies are similar as those observed in the literature [32] and reflect the extensivity character of the entropy functionals. Note that both Shannon and Rényi entropies describe appropriately the complexities associated to $1/f$ processes: maximum for highly disordered systems and minimum for smooth signals. For further information on wavelet entropy please refer to [30, 32].

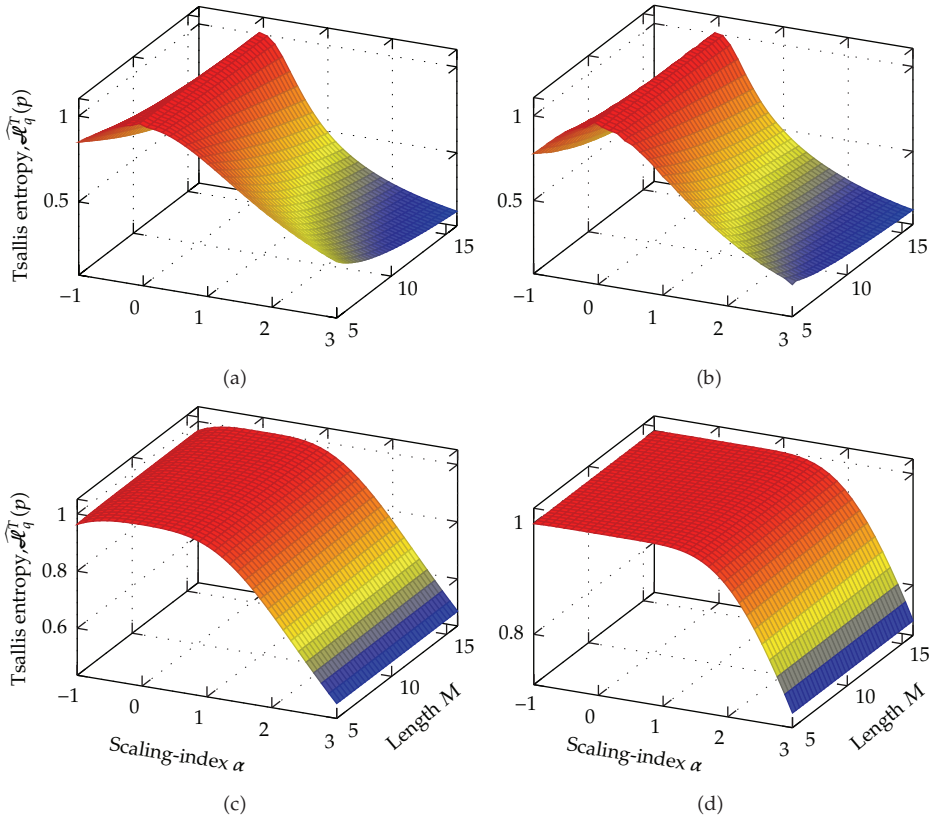

Figure 3: Wavelet Tsallis q-entropies of $1/f$ signals. Top left plot computed with $q = 0.4$, top right plot with $q = 0.95$, bottom left plot with $q = 5$, and finally bottom right plot with $q = 10$.

Figure 3 illustrates the wavelet Tsallis q-entropies for scaling processes of parameter α. Note that as long as $q < 5$, wavelet Tsallis q-entropies are identical as those observed in wavelet Rényi q-entropies (i.e., they have the same bell-shaped form). As long as $q \geq 5$, the behaviour of wavelet Tsallis q-entropies changes and differs from that of Shannon and Rényi. Wavelet Tsallis q-entropies, therefore, comprise the behaviour of wavelet Shannon and Rényi and provide greater flexibility in describing the process. Observe that, unlike Rényi entropies, Tsallis q-entropies allocate maximum (and constant) entropies to a set of scaling processes. In addition, the set of scaling signals for which this constant behaviour is observed is controlled by the nonextensivity parameter q of Tsallis entropies. The constant behaviour observed means that wavelet Tsallis q-entropies regard some set of scaling processes as totally random or disordered and, in some sense, randomizes the scaling signal under study. This particular behaviour of wavelet Tsallis q-entropies is further explored in next section, and a model for this is derived.

3.1. Sum-Cosh Window Behaviour of Wavelet Tsallis q-Entropies

Wavelet Tsallis q-entropies allocates constant entropies to a set of scaling processes and varying entropies to the rest. This particular behaviour can be modelled by the theory of

windowing or apodizing functions. This theory has been important for the design of digital filters; however, in this paper it is used to model the observed wavelet Tsallis q entropies of $1/f^{\alpha}$ signals. As a matter of fact, (3.8) resembles in some sense the cosh window observed in the work of Avci and Nacaroglu [39] and can be regarded as a sum-cosh window provided $\widehat{\mathscr{H}}_q^T(p;\alpha) = \widehat{\mathscr{H}}_q^T(p;-\alpha)$, $\lim_{\alpha\to 0}\widehat{\mathscr{H}}_q^T(p;\alpha) = 1$, and $\lim_{\alpha\to b}\widehat{\mathscr{H}}_q^T(p;\alpha) = 0$ conditions are satisfied. The symmetry condition ($\widehat{\mathscr{H}}_q^T(p;\alpha) = \widehat{\mathscr{H}}_q^T(p;-\alpha)$) is easily verified, and the $\lim_{\alpha\to 0}\widehat{\mathscr{H}}_q^T(p;\alpha)$ is computed based on the observation that

$$\mu_{\alpha} = \left(\frac{1-2^{\alpha}}{1-2^{\alpha M}}\right)^{q} = \left(\frac{-\alpha\ln 2 - (\alpha\ln 2)^2/2! - \cdots}{-\alpha M\ln 2 - (\alpha M\ln 2)^2/2! - \cdots}\right)^{q}, \tag{3.10}$$

which results in $\lim_{\alpha\to 0}\mu_{\alpha} = M^{-q}$. A similar reasoning for the expression to the right of μ_{α} in (3.6) results in

$$\lim_{\alpha\to 0}\widehat{\mathscr{H}}_q^T(p;\alpha) = c_{M,q}\left\{1 - \left(M^{-1}\right)^{q}M\right\} = 1. \tag{3.11}$$

Derivation of the second limit is performed by means of the asymptotic relation $1 - 2^{\alpha} \approx -2^{\alpha}$ for large α, consequently

$$\lim_{\alpha\to b}\widehat{\mathscr{H}}_q^T(p;\alpha) \approx c_{M,q}\left\{1 - \left(\frac{2^{\alpha}}{2^{\alpha M}}\right)^{q}\left(\frac{2^{\alpha M q}}{2^{\alpha q}}\right)\right\} = 0, \tag{3.12}$$

as b $\gg$ 1. The above demonstrates that wavelet Tsallis q-entropies can be modelled by sum-cosh windowing functions which in turn implies that for particular q, rectangular-like behaviour can be observed. The quasirectangular behaviour implies that constant regions of entropies are observed for a range of scaling processes and varying for the rest. The set of scaling processes for which constant wavelet Tsallis q-entropies are observed is controlled by the non-extensivity parameter q of Tsallis entropies. Figure 4 displays the shape of the wavelet Tsallis q-entropies for fixed length and different values of the non-extensivity parameter. For the cases $q = 0.999$ and $q = 3$, a bell-shaped form is observed which in some sense is identical to the ones observed for wavelet Shannon and Rényi entropies. Note from the figure that as $q = 8$, constant entropies are assigned to scaling processes in a symmetric range of α. This quasirectangular form can be set up to allocate constant entropies to stationary scaling processes and varying entropies to non-stationary ones. As a matter of fact, constant wavelet Tsallis entropies can be obtained for stationary signals and varying entropies to non-stationary ones as long as $q \approx 8$. This behaviour is important since a potential application of this feature is on the classification of scaling processes as stationary or non-stationary.

4. Classification of Scaling Signals

The classification of scaling signals as stationary or non-stationary has already been recognized as an important and unresolved problem in many areas of signal analysis [5, 12, 40–42]. Signal classification not only enhances the estimation process (i.e., estimation of the scaling index α) but also provides a correct interpretation of the phenomena, which in turn eases the application of a given technique in the process under study. Much of the literature

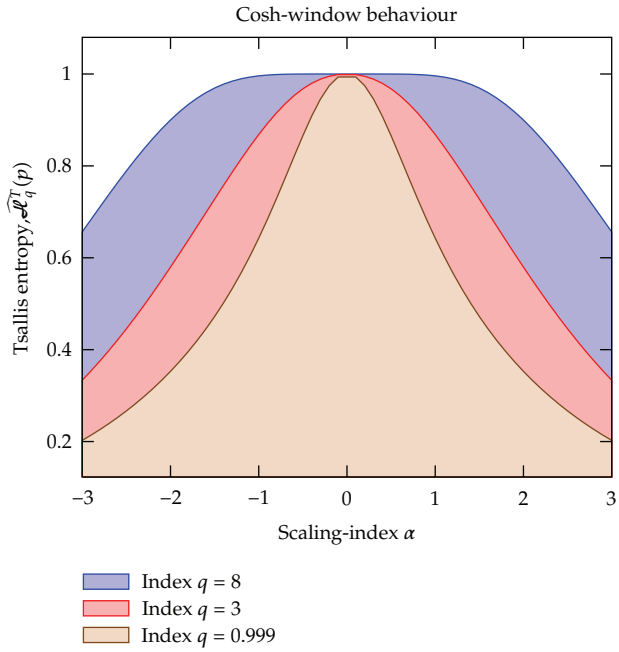

Figure 4: Cosh-window modelling of wavelet Tsallis q-entropies. Variation of window form on q.

on self-similar, long-memory, and fractal processes lack a step of signal classification, the parameters were estimated under the assumption of stationary, and therefore their results remain questionable. The process of signal classification becomes harder as we approach the boundary of stationarity and non-stationarity, that is, when $\alpha \to 1$. The reason for this is that as $\alpha \to 1$, stationary signals incorporate some features of non-stationarity and viceversa. Signal classification techniques often fail to distinguish fractal noises from motions within this boundary. The signal classification phase is sometimes more straightforward in some families of scaling signals than in others. For example, fBms and fGns are visually different, and the classification is simpler than that for the case of PPLs which are more difficult to classify. In this respect, any signal classification procedure must differentiate scaling signals independently of signal family and also provide meaningful classifications in the boundary $\alpha = 1$. Classification of scaling signals has traditionally been accomplished by using standard methodologies based on the PSD. PSD and PSD-based signal summation conversion (SSC) were recently proposed as methodologies for distinguishing fractal noises and motions in [5] by using synthesized fBms and fGns. In that work, fGns and fBms were generated in the interval $\alpha \in (-1, 3)$ and with sufficiently large lengths. The present paper proposes a methodology based on wavelet Tsallis q-entropies and its sum-cosh window behaviour. In the following, we briefly review current techniques employed to perform the signal classification phase and describe the proposed methodology based on wavelet Tsallis q-entropies.

4.1. Power Spectral Density

Spectral density function (SDF) characterizes stationary random signals in frequency domain. According to the work of Eke and coworkers [5, 41], SDF can be used to classify $1/f^{\alpha}$

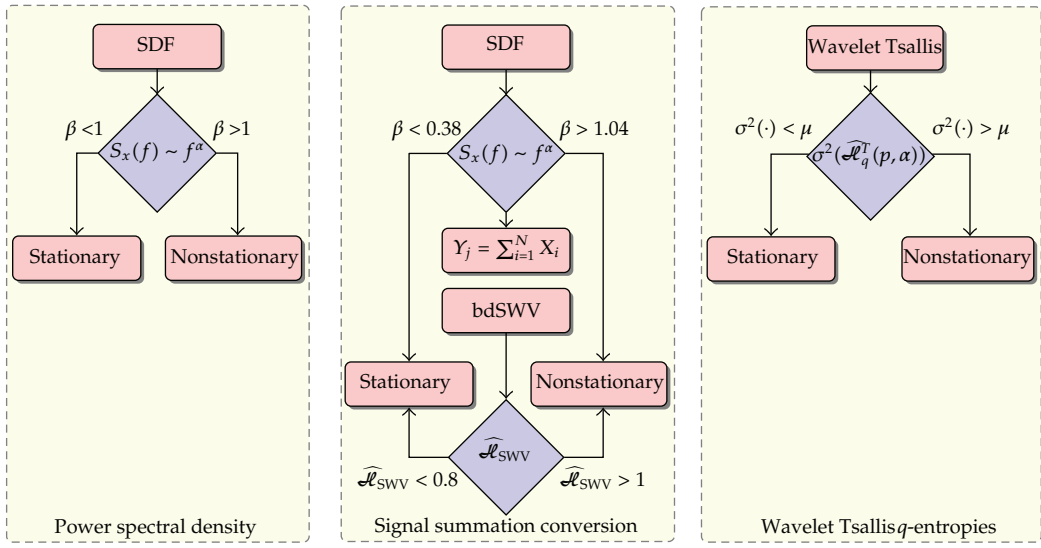

Figure 5: Algorithms for classifying scaling signals as stationary or nonstationary. Leftmost diagram displays the steps required in PSD, middle diagram the ones for SSC, and rightmost plot displays the steps of the proposed technique based on wavelet Tsallis q-entropies.

signals based on the fact that the observed PSD of $1/f$ processes follows a power-law dependence ($S_X(f) \sim f^{-\alpha}$). When the estimated parameter of power-law dependence ($\widehat{\alpha}$) is less than 1 ($\widehat{\alpha} < 1$), the process is stationary; on the other hand if $\widehat{\alpha} > 1$, the process is non-stationary. Signal classification in the SDF framework is therefore accomplished by first estimating the SDF of the scaling process under study using some standard methodology (e.g., Periodogram), plot $\log(S_x(f))$ versus f, fit a line, compute the slope which corresponds to the estimated $\widehat{\alpha}$, and finally based on the observed slope determine the nature of the process. Authors in [5] reported on the classification properties of the SDF method using synthesized signals of the fGn/fBm type. Eke and coauthors [5, 41] claimed that PSD performs satisfactorily when the process' scaling parameter lies in the intervals $-1 < \alpha < 0.38$ and $1.04 < \alpha < 3$ but misclassifies signals in the range $0.38 < \alpha < 1.04$. Because of this, they proposed a methodology specially designed to enhance the classification of signals in the interval $\alpha \in (-1, 3)$. Figure 5 displays the algorithm based on PSD to classify scaling signals.

4.2. Signal Summation Conversion

As stated in the previous section, PSD offers limited classification when the scaling process studied has a scaling index lying in the interval $\alpha \in (0.38, 1.04)$. The work of Eke et al. [5] not only identified this limitation but also proposed a solution based on the cumulative sum operation. The technique, called signal summation conversion, is only necessary whenever the estimated scaling index of the process lies in $\alpha \in (0.38, 1.04)$. The solution posed by Eke was to classify the process in the non-stationarity domain by the use of some standard non-stationarity technique. The use of the cumulative sum technique allowed the conversion of a stationary process into a non-stationary one and also maintaining the non-stationarity condition in a non-stationary process. Once the process to be classified is transformed to

exhibit non-stationarity features, the following step is to estimate the Hurst index of this process by using some standard technique, for example, bridge-detrended scaled-windowed variance (bdSWV). Depending upon the estimated Hurst index obtained by bdSWV ($\widehat{H}_{\mathrm{SWV}}$), a process is classified as stationary whenever $\widehat{H}_{\mathrm{SWV}} < 0.8$ and non-stationary when $\widehat{H}_{\mathrm{SWV}} > 1$. If the estimated $\widehat{H}_{\mathrm{SWV}}$ lies outside this interval, the scaling process is regarded as unclassifiable. Eke and coworkers showed that the SSC enhances the classification observed in PSD at the expense of higher computational time. Even though SSC enhanced the classification of processes, many disadvantages can be identified in this technique. First, extended fGn cannot be classified as stationary within this framework as its cumulative sum is still stationary; secondly, SSC is based on PSD, a technique which has traditionally been attached to stationary signals. In addition, SSC has not been tested on signals displaying more complex behaviour such as PPLs, and the signals used to perform the classification are long. Figure 5 displays the algorithms for performing scaling signal classification in the PSD and SSC framework.

4.3. Wavelet Tsallis q-Entropies

Section 3 demonstrated that wavelet Tsallis q-entropies can be modelled by sum-cosh apodizing functions which among other properties display constant regions of entropies and regions of decreasing entropies (i.e., quasirectangular behaviour). The length of the constant region, which usually lies in a symmetric range of the scaling index α, can be controlled by the non-extensivity parameter q of Tsallis entropies. If the constant region of entropies lies in the interval $\alpha \in (-1, 1)$, then, every stationary scaling process will present maximum wavelet Tsallis entropy ($\mathscr{H} = 1$). On the other hand if the process has a scaling index α outside this range it will present fluctuations of entropy. The above suggest that wavelet Tsallis q-entropies can be used to differentiate scaling signals as stationary or non-stationary based on the observed entropies. If the estimated entropies are constant, then the scaling process is stationary, otherwise it is non-stationary.

Figure 6 captures the rationale behind the signal classification procedure based on wavelet Tsallis q-entropies. As long as $q \geq 5$, constant regions of entropies are observed for scaling signals with $\alpha < \alpha_{\mathrm{coff}}(q)$ and varying for $\alpha > \alpha_{\mathrm{coff}}(q)$. If $\alpha_{\mathrm{coff}}(q) = 1$, then classification of fractional noises and motions can be accomplished, and when $\alpha_{\mathrm{coff}}(q) = 3$, classification of fractional motions from extended fractional motions is accomplished. Therefore, wavelet Tsallis q-entropies not only allows distinguishing stationary from non-stationary but also non-stationary from non-stationary.

5. Methodology

In [5], a comparison of PSD and SSC was performed by using synthesized signals of length $N = 2^{17}$. SSC was reported to present better classifications of fBms (as true fBms) and fGns (as true fGns). The present paper extends the results reported in [5] to PPL signals, which are known to present more complex behaviour than fBms and fGns, and proposes a novel methodology for scaling signal classification based on wavelet Tsallis q-entropies. The paper uses PPL signals with length $N = 2^{14}$, which are more realistic in the sense that many studies, reported in the literature with measured data, claimed that the nature of the phenomena does not permit to obtain higher signal lengths [6]. Also, estimation techniques often increase their MSE for short-length signals. Therefore, the present study not only proposes a methodology for classifying scaling processes as stationary or non-stationary but also compares the

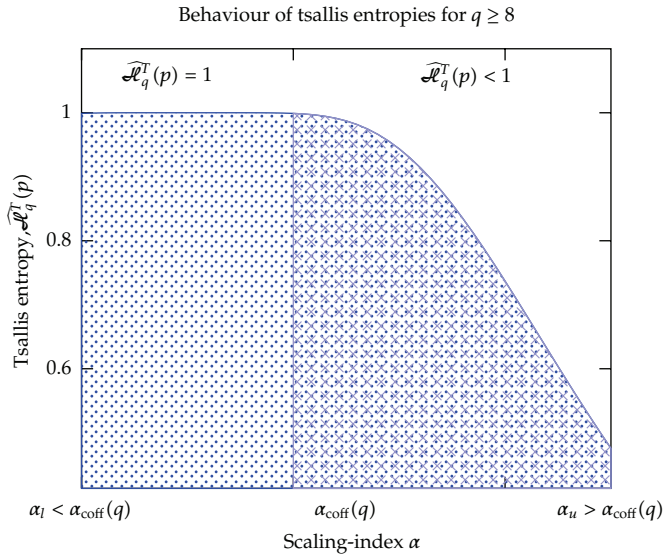

Figure 6: Dependence of the constant entropies on the nonextensivity parameter of Tsallis entropies.

techniques for signal classification in non-standard conditions (i.e., by using complex signals with short lengths). PPL signals were synthesized by using the R package `fractal`, which simulates signals using the circular embedding algorithm of Davies and Harte [43]. To test the performance of each technique, PPL signals were generated in the range $.01 < \alpha < 1.99$ in steps of .01. For each α (in the range $.01 < \alpha < 1.99$), 100 traces were simulated; therefore, a total of 19900 traces were studied. The selection of the range: $.01 < \alpha < 1.99$ is because of the fact that techniques of signal classification often fail in the limit $\alpha \to 1$ and perform better outside this range. SSC often considers a signal as unclassifiable; however, for the purposes of comparison, an unclassifiable signal is regarded as misclassified in this paper. SSC was implemented in R using the PSD algorithm of the `fractal` package. Wavelet entropy was implemented in R (and also in MATLAB), and the classification of signals was based on fluctuations of entropy (by computing wavelet entropy in sliding windows). To study the fluctuations, subsets of the original scaling signal, $X(t)$, were taken in sliding windows of the form:

$$X(m; w, \Delta) = X(t_k)\Pi\left(\frac{t - m\Delta}{w} - \frac{1}{2}\right), \tag{5.1}$$

where $m = 0, 1, 2, \ldots m_{\max}$, Δ is the sliding factor, and $\Pi(\cdot)$ is the standard rectangular function. Once the signals were classified, their results were summarized by plotting

$$\{\mathcal{N}(m; j), j\}_{j=.01}^{1.99}, \tag{5.2}$$

where $\mathcal{N}(m; j)$ stand for the number of signals classified correctly for the technique m for signals with scaling index j.

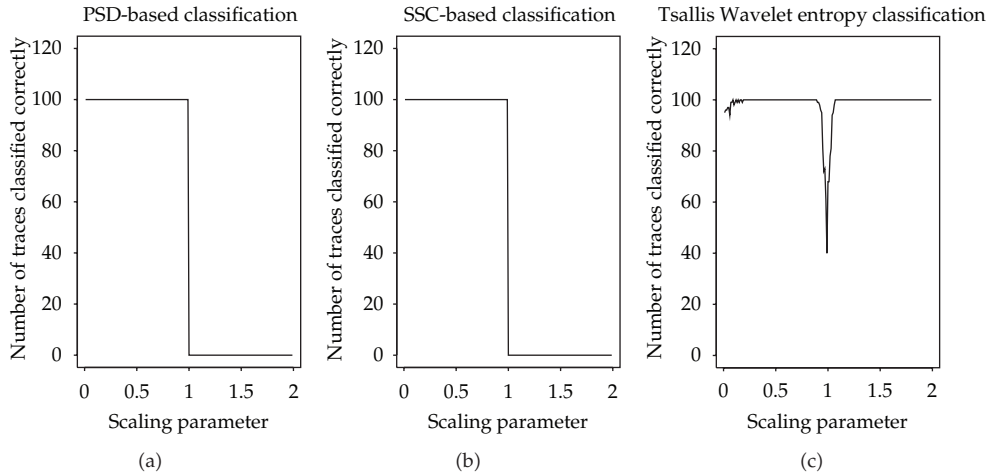

Figure 7: Classification of correct *power-law* signals. Recall that $\alpha < 1$ indicates the presence of a fractal noise while $\alpha > 1$ designates a non-stationary fractal motion. Left plot shows classification for PSD method, middle plot for the so-called SSC (signal summation conversion), and right plot to the novel wavelet Tsallis q-entropies-based method with $q = 20$.

6. Experimental Results

Figure 7 displays the results of the experimental study detailed (methodology) detailed in previous section. Note that for PSD, stationary PPL signals are classified correctly (i.e., classified as stationary). This was expected, since as previously stated, PSD was primarily designed to work for time-invariant (stationary) random signals. For non-stationary signals, PSD classifies non-stationary signals as stationary, misclassifying every non-stationary PPL process. PSD, therefore, do not provide reliable classifications of PPL signals, and it is not recommended for use in a signal classification scheme. In [5], SSC was shown to enhance the classification of scaling signals for the range $\widehat{\alpha} \in (0.38, 1.04)$. Note, however, that SSC enhances the classification mostly for stationary signals. Moreover, SSC is only applicable as the estimated scaling index lies in $\widehat{\alpha} \in (0.38, 1.04)$, otherwise only the PSD is applied. Based on this, it is expected to have a similar behaviour of classifications as the PSD for the SSC technique. Middle plot of Figure 7 displays the classifications of the SSC technique for PPL signals of length $N = 2^{14}$. As expected, SSC presents identical behaviour as that of PSD and, as the case of PSD, is not recommended as a signal classification tool for signals with PPL behaviour. The results of PSD and those of SSC differ from those presented in [5]. Note, however, that the signals studied in this paper are of different nature than those studied in [5]. First, the signals studied in the work of Eke et al. [5] are fBms and fGns, which in some sense are more easily classifiable since their smoothness properties are visually different. Finally, the length of the signals studied in the work of Eke are longer than the length of the signals considered in this paper. It is well known that as the length of the studied signals increases, the MSE of the estimated $\widehat{\alpha}$ decreases. Thus, the synthesized signals studied in this paper possess not only higher complexities but also shorter length. Rightmost plot of Figure 7 presents the classifications of PPL signals using the methodology proposed in this paper based on wavelet Tsallis q-entropies. Note that the classifications of the proposed technique are better than those observed in PSD and SSC. The proposed technique based on wavelet Tsallis q-entropies classifies correctly stationary as well as non-stationary PPL signals and that this classification

is somewhat unacceptable in the limit of $\alpha \to 1$. The technique based on wavelet Tsallis q-entropies is fast enough and can also classify extended fGns from fGns and fBms from extended fBms. The classifications of signals with these characteristics are not supported by either the PSD and SSC techniques. In performing the classifications with the technique based on wavelet Tsallis entropies, the entropies were computed in sliding windows, and the boundary of fluctuations was taken as $\mu = 3e - 09$. The nonextensivity parameter q was set to $q = 10$ but similar results are observed for $q \geq 10$.

7. Conclusions

This paper presented a novel methodology for classifying scaling signals as stationary or non-stationary based on wavelet Tsallis q-entropies. It was shown that the sum-cosh window behaviour of wavelet Tsallis q-entropies allocated constant entropies to a set of scaling signals and varying to the rest and that the length of the constant region is controlled by q, the non-extensivity parameter of Tsallis entropies. It was also shown that by setting the constant regions to the range of stationary scaling signals, the problem of signal classification can be reduced to the observation of constant/nonconstant entropies. The classification properties of the PSD and SSC were extended to signals with pure power-law behaviour with length $N = 2^{14}$, and a comparison procedure was performed among PSD, SSC, and the technique based on wavelet Tsallis q-entropy. The results not only confirm that the technique based on wavelet Tsallis q-entropies provides meaningful classification but also outperforms PSD and SSC techniques. The results presented in this paper are meaningful in many areas of scaling signal analysis since many estimation/analysis results presented in the literature have been performed without a phase of signal classification.

Acknowledgments

The present paper was jointly funded by the National Council of Science and Technology (CONACYT) under Grant 47609, FOMIX-COQCYT Grant no. 126031, and University of Caribe internal funds.

References

[1] J. Beran, "Statistical methods for data with long-range dependence (with discussion)," *Statistical Science*, vol. 7, pp. 404–416, 1992.
[2] J. Beran, *Statistics for Long-Memory Processes*, vol. 61 of *Monographs on Statistics and Applied Probability*, Chapman & Hall, New York, NY, USA, 1994.
[3] G. Samorodnitsky and M. S. Taqqu, *Stable Non-Gaussian Random Processes*, Stochastic Modeling, Chapman & Hall, New York, NY, USA, 1994.
[4] M. J. Cannon, D. B. Percival, D. C. Caccia, G. M. Raymond, and J. B. Bassingthwaighte, "Evaluating scaled windowed variance methods for estimating the Hurst coefficient of time series," *Physica A*, vol. 241, no. 3-4, pp. 606–626, 1997.
[5] A. Eke, P. Hermán, J. B. Bassingthwaighte et al., "Physiological time series: distinguishing fractal noises from motions," *Pflugers Archiv European Journal of Physiology*, vol. 439, no. 4, pp. 403–415, 2000.
[6] D. Delignieres, S. Ramdani, L. Lemoine, K. Torre, M. Fortes, and G. Ninot, "Fractal analyses for "short" time series: a re-assessment of classical methods," *Journal of Mathematical Psychology*, vol. 50, no. 6, pp. 525–544, 2006.
[7] W. E. Leland, M. S. Taqqu, W. Willinger, and D. V. Wilson, "On the self-similar nature of Ethernet traffic (extended version)," *IEEE/ACM Transactions on Networking*, vol. 2, no. 1, pp. 1–15, 1994.
[8] I. W. C. Lee and A. O. Fapojuwo, "Stochastic processes for computer network traffic modeling," *Computer Communications*, vol. 29, no. 1, pp. 1–23, 2005.

[9] D. B. Percival, "Stochastic models and statistical analysis for clock noise," *Metrologia*, vol. 40, no. 3, pp. S289–S304, 2003.
[10] S. B. Lowen and M. C. Teich, "Estimation and simulation of fractal stochastic point processes," *Fractals*, vol. 3, no. 1, pp. 183–210, 1995.
[11] S. Thurner, S. B. Lowen, M. C. Feurstein, C. Heneghan, H. G. Feichtinger, and M. C. Teich, "Analysis, synthesis, and estimation of fractal-rate stochastic point processes," *Fractals*, vol. 5, no. 4, pp. 565–595, 1997.
[12] D. C. Caccia, D. Percival, M. J. Cannon, G. Raymond, and J. B. Bassingthwaighte, "Analyzing exact fractal time series: evaluating dispersional analysis and rescaled range methods," *Physica A*, vol. 246, no. 3-4, pp. 609–632, 1997.
[13] F. Serinaldi, "Use and misuse of some Hurst parameter estimators applied to stationary and non-stationary financial time series," *Physica A*, vol. 389, no. 14, pp. 2770–2781, 2010.
[14] B. D. Malamud and D. L. Turcotte, "Self-affine time series: measures of weak and strong persistence," *Journal of Statistical Planning and Inference*, vol. 80, no. 1-2, pp. 173–196, 1999.
[15] J. C. Gallant, I. D. Moore, M. F. Hutchinson, and P. Gessler, "Estimating fractal dimension of profiles: a comparison of methods," *Mathematical Geology*, vol. 26, no. 4, pp. 455–481, 1994.
[16] W. Rea, M. Reale, J. Brown, and L. Oxley, "Long memory or shifting means in geophysical time series?" *Mathematics and Computers in Simulation*, vol. 81, no. 7, pp. 1441–1453, 2011.
[17] C. Cappelli, R. N. Penny, W. S. Rea, and M. Reale, "Detecting multiple mean breaks at unknown points in official time series," *Mathematics and Computers in Simulation*, vol. 78, no. 2-3, pp. 351–356, 2008.
[18] B. B. Mandelbrot and J. W. van Ness, "Fractional Brownian motions, fractional noises and applications," *SIAM Review*, vol. 10, pp. 422–437, 1968.
[19] P. Flandrin, "Wavelet analysis and synthesis of fractional Brownian motion," *IEEE Transactions on Information Theory*, vol. 38, no. 2, part 2, pp. 910–917, 1992.
[20] S. Stoev, M. S. Taqqu, C. Park, and J. S. Marron, "On the wavelet spectrum diagnostic for Hurst parameter estimation in the analysis of Internet traffic," *Computer Networks*, vol. 48, no. 3, pp. 423–445, 2005.
[21] L. Hudgins, C. A. Friehe, and M. E. Mayer, "Wavelet transforms and atmopsheric turbulence," *Physical Review Letters*, vol. 71, no. 20, pp. 3279–3282, 1993.
[22] A. Cohen and A. J. Kovačević, "Wavelets: the mathematical background," *Proceedings of the IEEE*, vol. 84, no. 4, pp. 514–522, 1996.
[23] P. Abry and D. Veitch, "Wavelet analysis of long-range-dependent traffic," *IEEE Transactions on Information Theory*, vol. 44, no. 1, pp. 2–15, 1998.
[24] H. Shen, Z. Zhu, and T. C. M. Lee, "Robust estimation of the self-similarity parameter in network traffic using wavelet transform," *Signal Processing*, vol. 87, no. 9, pp. 2111–2124, 2007.
[25] J.-M. Bardet, "Statistical study of the wavelet analysis of fractional Brownian motion," *IEEE Transactions on Information Theory*, vol. 48, no. 4, pp. 991–999, 2002.
[26] J. A. Bonachela, H. Hinrichsen, and M. A. Muñoz, "Entropy estimates of small data sets," *Journal of Physics A*, vol. 41, no. 20, Article ID 202001, 2008.
[27] U. Kumar, V. Kumar, and J. N. Kapur, "Normalized measures of entropy," *International Journal of General Systems*, vol. 12, no. 1, pp. 55–69, 1986.
[28] M. T. Martin, A. R. Plastino, and A. Plastino, "Tsallis-like information measures and the analysis of complex signals," *Physica A*, vol. 275, no. 1, pp. 262–271, 2000.
[29] R. G. Baraniuk, P. Flandrin, A. J. E. M. Janssen, and O. J. J. Michel, "Measuring time-frequency information content using the Rényi entropies," *IEEE Transactions on Information Theory*, vol. 47, no. 4, pp. 1391–1409, 2001.
[30] D. G. Pérez, L. Zunino, M. Garavaglia, and O. A. Rosso, "Wavelet entropy and fractional Brownian motion time series," *Physica A*, vol. 365, no. 2, pp. 282–288, 2006.
[31] M. M. Añino, M. E. Torres, and G. Schlotthauer, "Slight parameter changes detection in biological models: a multiresolution approach," *Physica A*, vol. 324, no. 3-4, pp. 645–664, 2003.
[32] L. Zunino, D. G. Pérez, M. Garavaglia, and O. A. Rosso, "Wavelet entropy of stochastic processes," *Physica A*, vol. 379, no. 2, pp. 503–512, 2007.
[33] R. Quian Quiroga, O. A. Rosso, E. Başar, and M. Schürmann, "Wavelet entropy in event-related potentials: a new method shows ordering of EEG oscillations," *Biological Cybernetics*, vol. 84, no. 4, pp. 291–299, 2001.
[34] W. X. Ren and Z. S. Sun, "Structural damage identification by using wavelet entropy," *Engineering Structures*, vol. 30, no. 10, pp. 2840–2849, 2008.

[35] H. A. Al-Nashash, J. S. Paul, W. C. Ziai, D. F. Hanley, and N. V. Thakor, "Wavelet entropy for subband segmentation of EEG during injury and recovery," *Annals of Biomedical Engineering*, vol. 31, no. 6, pp. 653–658, 2003.

[36] O. A. Rosso, L. Zunino, D. G. Pérez et al., "Extracting features of Gaussian self-similar stochastic processes via the Bandt-Pompe approach," *Physical Review E*, vol. 76, no. 6, Article ID 061114, 6 pages, 2007.

[37] L. Zunino, D. G. Pérez, M. T. Martín, A. Plastino, M. Garavaglia, and O. A. Rosso, "Characterization of Gaussian self-similar stochastic processes using wavelet-based informational tools," *Physical Review E*, vol. 75, no. 2, Article ID 021115, 10 pages, 2007.

[38] D. G. Pérez, L. Zunino, M. T. Martín, M. Garavaglia, A. Plastino, and O. A. Rosso, "Model-free stochastic processes studied with q-wavelet-based informational tools," *Physics Letters, Section A*, vol. 364, no. 3-4, pp. 259–266, 2007.

[39] K. Avci and A. Nacaroglu, "Cosh window family and its application to FIR filter design," *AEU*, vol. 63, no. 11, pp. 907–916, 2009.

[40] P. Castiglioni, G. Parati, A. Civijian, L. Quintin, and M. D. Rienzo, "Local scale exponents of blood pressure and heart rate variability by detrended fluctuation analysis: effects of posture, exercise, and aging," *IEEE Transactions on Biomedical Engineering*, vol. 56, no. 3, Article ID 4633671, pp. 675–684, 2009.

[41] A. Eke, P. Hermán, L. Kocsis, and L. R. Kozak, "Fractal characterization of complexity in temporal physiological signals," *Physiological Measurement*, vol. 23, no. 1, pp. R1–R38, 2002.

[42] G. L. Gebber, H. S. Orer, and S. M. Barman, "Fractal noises and motions in time series of presympathetic and sympathetic neural activities," *Journal of Neurophysiology*, vol. 95, no. 2, pp. 1176–1184, 2006.

[43] R. B. Davies and D. S. Harte, "Tests for hurst effect," *Biometrika*, vol. 74, no. 1, pp. 95–101, 1987.